Alexandria Engineering Journal (2016) 55, 2171–2181

HOSTED BY

ELSEVIER

Alexandria University

Alexandria Engineering Journal

www.elsevier.com/locate/aej
www.sciencedirect.com

ORIGINAL ARTICLE

Heat transfer analysis of Jeffery fluid flow over a stretching sheet with suction/injection and magnetic dipole effect

A. Zeeshan *, **A. Majeed**

Department of Mathematics and Statistics, FBAS, International Islamic University, Islamabad, Pakistan

Received 9 February 2016; revised 3 June 2016; accepted 9 June 2016
Available online 27 June 2016

KEYWORDS

Jeffery fluid;
Magnetic dipole;
Stretching surface;
Prescribed heat flux;
Suction/injection

Abstract The purpose of the present paper was to investigate the flow and heat transfer of Jeffery fluid past a linearly stretching sheet with the effect of a magnetic dipole. The governing differential equations of motion and heat transfer are transformed into nonlinear coupled ordinary differential equations (ODEs) using appropriate similarity transformations. Then the ODEs are solved by adopting two different schemes, Runge–Kutta with shooting technique and series solution based on GA and NM. The effect of various physical parameters including ferromagnetic interaction parameter (β), Deborah number (γ_1), Prandtl number (Pr), suction/injection parameter (S), ratio of relaxation to retardation times (λ_2) on velocity and temperature profiles is illustrated graphically and in tabular form by considering two types of thermal process namely prescribed surface temperature (PST) and prescribed heat flux (PHF). Comparison with available results for particular cases is found an excellent agreement.

1. Introduction

Boundary layer flow and heat and mass transfer over a stretching surface have received spectacular attention due to their extensive applications in industry, engineering, and metallurgy process such as production of polythene and paper, polymer extrusion, cooling of elastic sheets, wire drawing, fiber technology, continuous stretching of plastic films, hot rolling, crystal growing and cooling of an infinite metallic plate in a cooling bath. Heat transfer is important because the rate of cooling can be controlled and final products of desired characteristics might be achieved. Flow over a flat plate with uniform free stream has been examined by Blasius [1]. The boundary layer flow over a continuous moving flat surface was initially investigated by Sakiadis [2]. Crane [3] established a simple closed form analytical solution for two-dimensional incompressible boundary layer flow over a linear stretching sheet with the velocity proportional to the distance from the origin. This problem was extended to heat and mass transfer with the effect of suction or blowing by Gupta and Gupta [4]. Ariel [5] considered the problem of boundary layer flow of a viscous fluid by a stretching sheet using homotopy perturbation method. Some of the collections of research papers existing in the open literature can be found in [6–11].

* Corresponding author.
E-mail addresses: ahmad.zeeshan@iiu.edu.pk (A. Zeeshan), Mjaaqib@yahoo.com (A. Majeed).

Peer review under responsibility of Faculty of Engineering, Alexandria University.

http://dx.doi.org/10.1016/j.aej.2016.06.014

Nomenclature

a	distance
c	stretching rate (s^{-1})
c_p	specific heat at constant pressure ($Jkg^{-1}\ K^{-1}$)
C_f	skin friction coefficient
f	dimensionless stream function
H	magnetic field (A/m)
k	thermal conductivity ($Wm^{-1}\ K^{-1}$)
K^*	pyromagnetic coefficient
κ	extra stress tensor
M	magnetization (A/m)
N_{ux}	local Nusselt number
Pr	Prandtl number
Re_x	local Reynolds number
R_1	Rivlin-Ericksen tensor
S	suction/injection parameter
T	temperature (K)
T_c	Curie temperature (K)
(u,v)	velocity components ($m\ s^{-1}$)
(x, y)	coordinates along and normal to sheet (m)
μ	dynamic viscosity ($Ns\ m^{-1}$)
μ_o	magnetic permeability
θ	dimensionless temperature

Greek symbols

α_1	dimensionless distance
β	ferromagnetic interaction parameter
γ	magnetic field strength (A/m)
γ_1	Deborah number
ρ	density ($kg\ m^{-3}$)
ε	dimensionless curie temperature
(η,ξ)	dimensionless coordinate
ψ	stream function ($m^2\ s^{-1}$)
ϕ	magnetic potential
τ	Cauchy stress tensor
λ	viscous dissipation parameter
$\lambda_1\ \lambda_2$	material parameters of Jeffrey fluid

However, all the above-mentioned researches are restricted to Newtonian fluid flows. Fluids that do not obey the Newton's law of motion are called non-Newtonian fluids. Study of non-Newtonian fluids has received great attention in modern technologies such as geothermal engineering, geophysical, astrophysical bio-fluid and petroleum industries, and some of the examples of non-Newtonian fluids are toothpaste, waste fluids, and food products. Many constituent relations of non-Newtonian fluids have been considered in the literature due to its versatile nature. Here we considered Jeffrey fluid model for non-Newtonian fluids. Sahoo [12] performed heat transfer analysis of non-Newtonian fluid over a stretching surface. He applied finite difference method with shooting technique to obtain simultaneous effects of the partial slip and the third-grade fluid parameter on velocity and temperature fields.

Sandeep et al. [13] investigated the stagnation point flow of MHD Jeffrey nanofluid over a stretching surface with induced magnetic field and chemical reaction. Raju et al. [14] analyzed the effects of nonlinear thermal radiation on 3D Jeffrey fluid flow over a stretching/shrinking surface in the presence of homogeneous-heterogeneous reactions, non-uniform heat source/sink, and suction/injection. Rashidi et al. [15] performed mixed convective laminar, incompressible flow and heat analysis transfer of viscoelastic fluid over a permeable wedge with thermal radiation by employing homotopy analysis method (HAM).

Hayat et al. [16] considered Jeffery fluid flow in a porous channel in the presence of a transverse magnetic field. They found a semi-analytical solution to the highly nonlinear problem by applying HAM. Hayat et al. [17] determined three-dimensional boundary layer flow of Jeffrey fluid past a stretching surface by employing HAM. Animasaun et al. [18] studied the motion of viscoelastic fluid toward a stretching sheet in the presence of induced magnetic field for the case of unequal diffusivities of homogeneous–heterogeneous reaction with thermal radiation. Nadeem et al. [19] investigated the effect of nanoparticles on two-dimensional steady flow of a Jeffrey fluid past a stretching surface. Rashidi and Erfani [20] analyzed thermal-diffusion and soret effect on steady MHD convective slip flow due to a rotating disk with viscous dissipation and Ohmic heating using the DTM-Padé technique.

Malik et al. [21] presented the Jeffrey fluid flow with a pressure-dependent viscosity. They considered two types of flow problem, Couette and Poiseulle flow for the Jeffrey fluid. Raju et al. [22] have discussed MHD chemically reacting boundary layer flow of Jeffrey nanofluid over a permeable cone in a porous medium with the effect of thermophoresis, Brownian motion, and thermal radiation. Sandeep et al. [23] studied heat and mass transfer of convective non-Newtonian nanofluids over a permeable stretching sheet with the effects of transverse magnetic field and suction/injection. Abolbashari et al. [24] examined entropy analysis for MHD nano-fluid past a permeable stretching surface. They considered four different types of nanoparticles with water as the base fluid. Narayana et al. [25] studied the flow of micropolar ferromagnetic fluid due to stretching of an elastic sheet in the presence of an applied magnetic field.

In view of all the above-stated application, the main objective of the present article was to explore the flow and heat transfer behavior of Jeffery fluid over a stretching surface with the influence of magnetic dipole. Effect of non-dimensional governing parameters such as ferromagnetic interaction parameter, suction/injection parameter, Deborah number, the ratio of relaxation to retardation times, Prandtl number on velocity and temperature fields is analyzed through the graph.

2. Mathematical formulation

2.1. Magnetic dipole

Magnetic liquid flow is influenced by the dipole field whose permanent magnetic scalar potential is taken as

$$\Phi = \frac{\gamma}{2\pi}\left(\frac{x}{x^2+(y+a)^2}\right), \tag{1}$$

where γ is the strength of magnetic field. The components of magnetic field intensity H_x and H_y along the coordinates x and y axes are

$$H_x = -\frac{\partial \Phi}{\partial x} = \frac{\gamma}{2\pi}\left\{\left(\frac{x^2-(y+a)^2}{\left(x^2+(y+a)^2\right)^2}\right)\right\}, \tag{2}$$

$$H_y = -\frac{\partial \Phi}{\partial y} = \frac{\gamma}{2\pi}\left\{\left(\frac{2x(y+a)}{\left(x^2+(y+a)^2\right)^2}\right)\right\}, \tag{3}$$

The resultant magnitude H of the magnetic field intensity is given by

$$H = \left[\left(\frac{\partial \Phi}{\partial x}\right)^2 + \left(\frac{\partial \Phi}{\partial y}\right)^2\right]^{\frac{1}{2}}, \tag{4}$$

$$\frac{\partial H}{\partial x} = -\frac{\gamma}{2\pi}\left(\frac{2x}{(y+a)^4}\right), \tag{5}$$

$$\frac{\partial H}{\partial y} = \frac{\gamma}{2\pi}\left(\frac{-2}{(y+a)^3} + \frac{4x^2}{(y+a)^5}\right), \tag{6}$$

The variation of magnetization M can be considered as a linear function of temperature [26].

$$M = K^*(T_c - T), \tag{7}$$

where K^* is a pyromagnetic coefficient and T_c is the Curie temperature; however, the following point is essential for the occurrence of ferrohydrodynamic interaction: (i) the fluid is at a temperature T different from T_c and (ii) the external magnetic field is inhomogeneous. Once the ferromagnetic fluid approaches Curie temperature, there is no furthermore magnetization. Characteristic for physical significance is very important , as Curie temperature is very high, that is 1043 K for iron.

2.2. Flow analysis

Let us consider a two-dimensional viscous incompressible flow of Jeffrey fluid, electrically non-conducting past a stretching surface under the impact of the magnetic field induced by the magnetic dipole. A stretching sheet is considered along the x-axis with velocity $u_w = cx$ and y-axis is normal to it as shown schematically in Fig. 1. A magnetic dipole is situated in the center of y-axis and distance "a" from the sheet. Due to a dipole, magnetic field points in the positive x-direction and rises the magnetic field strength to marinate the ferrofluid. It is also supposed that the uniform temperature at the surface is T_w and Curie temperature T_c, while the temperature of the ambient ferrofluid far from the surface of the sheet is $T_\infty = T_c$ and unable to magnetize until they start to cool after coming into the thermal boundary layer area near to the sheet.

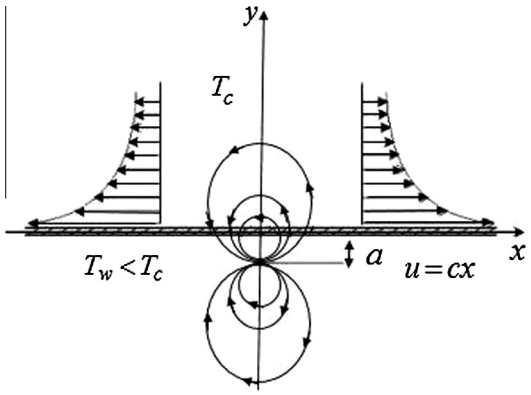

Figure 1 The geometry of the problem, circles indicate magnetic dipole.

The necessary equations for Jeffrey model can be written as [27]

$$\tau = pI + \kappa \tag{8}$$

$$\kappa = \frac{\mu}{1+\lambda_2}\left[R_1 + \lambda_1\left(\frac{\partial R_1}{\partial t} + V\cdot\nabla\right)R_1\right] \tag{9}$$

where τ is the Cauchy stress tensor, κ is extra stress tensor, μ is the dynamic viscosity λ_2 and λ_1 are material parameters of Jeffrey fluid and R_1 is the Rivlin-Ericksen tensor defined by

$$R_1 = (\nabla V) + (\nabla V)' \tag{10}$$

Using the boundary layer approximation, the continuity and momentum equations of Jeffery fluid are listed below:

$$\frac{\partial u}{\partial x} + \frac{\partial v}{\partial y} = 0, \tag{11}$$

$$u\frac{\partial u}{\partial x} + v\frac{\partial u}{\partial y} = \frac{\mu_0}{\rho}M\frac{\partial H}{\partial x} + \frac{\nu}{1+\lambda_2}\left[\frac{\partial^2 u}{\partial y^2} + \lambda_1\left(u\frac{\partial^3 u}{\partial x \partial y^2} + v\frac{\partial^3 u}{\partial y^3} - \frac{\partial u}{\partial x}\frac{\partial^2 u}{\partial y^2} + \frac{\partial u}{\partial y}\frac{\partial^2 u}{\partial x \partial y}\right)\right], \tag{12}$$

where (u, v) are the velocity components along the (x, y) directions, respectively. λ_1 is the relaxation time, λ_2 is the ratio of relaxation to the retardation times, ρ is the density of the fluid, μ is the dynamic viscosity, $\nu = \frac{\mu}{\rho}$ is the kinematic viscosity, μ_0 is the magnetic permeability, k is the thermal conductivity, c_P is specific heat, M is the magnetization, and H is the magnetic field.

The relevant boundary conditions on velocity profile are

$$u = u_w = cx, \quad v = v_w, \text{ at } y = 0 \tag{13}$$

$$u \to 0, \quad \frac{\partial u}{\partial y} \to 0, \text{ as } y \to \infty$$

where $c > 0$ is stretching rate of sheet, and v_w is the suction/injection velocity.

To solve the governing Eq. (12), following similarity transformations are used [26]

$$\Psi(\xi,\eta) = \left(\frac{\mu}{\rho}\right)\xi\cdot f(\eta), \quad \xi = \sqrt{\frac{c\mu}{\rho}}x, \quad \eta = \sqrt{\frac{c\mu}{\rho}}y \tag{14}$$

$\Psi(\xi, \eta)$ is the stream function and ξ, η are the dimensionless coordinates (15)

The velocity components can be defined as

$$u = \frac{\partial \Psi}{\partial y} = cx\cdot f'(\eta), \quad v = -\frac{\partial \Psi}{\partial x} = -\sqrt{c\nu}\cdot f(\eta) \tag{16}$$

Substituting Eq. (16) in Eq. (12), and comparing the coefficients of like powers up to order ξ^2, we get the fourth-order nonlinear ordinary differential equations:

$$f''' - (1+\lambda_2)(f'^2 - ff'') + \gamma_1(f''^2 - ff^{iv}) - (1+\lambda_2)\frac{2\beta\theta_1}{(\eta+\alpha_1)^4} = 0, \tag{17}$$

In view of the transformations, Eq. (13) takes the following non-dimensional form

$$f = S, \quad f' = 1 \text{ at } \eta = 0 \tag{18}$$

$$f' \to 0, \quad f'' \to 0 \text{ as } \eta \to \infty$$

Here $\gamma_1 = \lambda_1 c$ is the Deborah number and $\beta = \frac{\gamma\rho}{2\pi\mu^2}\mu_0 K^*(T_c - T_w)$ is the ferromagnetic interaction parameter, $S = \frac{-v_w}{\sqrt{cv}}$ is the suction/injection parameter with $S > 0$ for suction and $S < 0$ for injection.

2.3. Heat transfer

The energy equation with the existence of magnetic fluid and viscous dissipation is given by [28]

$$\rho c_p\left(u\frac{\partial T}{\partial x} + v\frac{\partial T}{\partial y}\right) + \mu_0 T\frac{\partial M}{\partial T}\left(u\frac{\partial H}{\partial x} + v\frac{\partial H}{\partial y}\right) = k\frac{\partial^2 T}{\partial y^2} + \mu\left(\frac{\partial u}{\partial y}\right)^2 + 2\mu\left(\frac{\partial v}{\partial y}\right)^2 \tag{19}$$

where ρ is the density of the fluid, c_P is specific heat, μ_0 is the magnetic permeability, k is the thermal conductivity and T is the fluid temperature.

To solve the thermal boundary layer Eq. (8), we consider non-isothermal temperature boundary condition as

$$\left.\begin{aligned} T &= T_w = T_c - A\left(\tfrac{x}{l}\right)^2 \quad \text{for PST} \\ q_w &= -k\tfrac{\partial T}{\partial y} = D\left(\tfrac{x}{l}\right)^2 \quad \text{for PHF} \end{aligned}\right\} \quad \text{at } y = 0 \tag{20}$$

$$T \to T_c, \text{ as } y \to \infty$$

where A and D are positive constants and $l = \sqrt{v/c}$ is the characteristic length.

Now we introduce the dimensionless variable $\theta(\xi, \eta)$

$$\theta(\xi,\eta) \equiv \frac{T_c - T}{T_c - T_w} = \theta_1(\eta) + \xi^2\theta_2(\eta), \tag{21}$$

where

$T_c - T_w = A\left(\tfrac{x}{l}\right)^2$ for PST, $T_c - T_w = \frac{D}{k}\left(\tfrac{x}{l}\right)^2\sqrt{\tfrac{v}{c}}$ for PHF

Substituting Eq. (21) in Eq. (19) we obtain non-dimensional thermal boundary layer equations up to order ξ^2

$$\theta_1'' + Pr(f\theta_1' - 2f'\theta) + \frac{2\lambda\beta(\theta_1 - \varepsilon)f}{(\eta+\alpha_1)^3} - 2\lambda f'^2 = 0, \tag{22}$$

$$\theta_2'' - Pr(4f'\theta_2 - f\theta_2') + \frac{2\lambda\beta\theta_2 f}{(\eta+\alpha_1)^3} - \lambda\beta(\theta_1 - \varepsilon)\left[\frac{2f'}{(\eta+\alpha_1)^4} + \frac{4f}{(\eta+\alpha_1)^5}\right] - \lambda f''^2 = 0, \tag{23}$$

where $Pr = \frac{\mu c_p}{k}$ is Prandtl number, $\lambda = \frac{c\mu^2}{\rho k(T_c - T_w)}$ λ is the viscous dissipation parameter, $\alpha_1 = \sqrt{\frac{c\rho}{\mu}}a$ is the dimensionless distance from the origin to the magnetic dipole and $\varepsilon = \frac{T_c}{T_c - T_w}$ is the dimensionless Curie temperature ratio.

The boundary conditions (20) become

$$\left.\begin{aligned} \theta_1 &= 1, \quad \theta_2 = 0, \quad \text{for PST} \\ \theta_1' &= -1, \quad \theta_2' = 0, \quad \text{for PHF} \end{aligned}\right\} \text{ at } \eta = 0 \tag{24}$$

$$\theta_1 \to 0, \quad \theta_2 \to 0, \text{ as } \eta \to \infty$$

The quantities of physical interest are the local skin-friction coefficient and the local Nusselt number can be expressed as

$$C_{f_x} \equiv \frac{-2\tau_w}{\rho(cx)^2}, \quad Nu_x \equiv \frac{xq_w}{-k(T_c - T_w)} \tag{25}$$

where τ_w is the surface shear stress and q_w is the surface heat flux are

$$\tau_w = \mu\left(\frac{\partial u}{\partial y}\right)_{y=0}, \quad q_w = -\left(\frac{\partial T}{\partial y}\right)_{y=0} \tag{26}$$

Using Eqs. (16) and (21) we have

$$\left.\begin{aligned} C_f Re_x^{1/2} &= -2f''(0), \\ Nu_x/Re_x^{1/2} &= -(\theta_1'(0) + \xi^2\theta_2'(0)) \text{ PST} \\ Nu_x/Re_x^{1/2} &= 1/(\theta_1(0) + \xi^2\theta_2(0)) \text{ PHF} \end{aligned}\right\}, \tag{27}$$

where $Re_x = \frac{\rho c x^2}{\mu}$ is the local Reynolds number. It is superficial that the flow is influenced by the ferromagnetic parameter β. It is more fascinating and suitable to exchange the dimensionless wall heat transfer rate $-\theta' = -[\theta_1'(0) + \xi^2\theta_2'(0)]$ by the independent of the distance ξ, a ratio $\theta^*(0) = \frac{\theta_1'(0)}{\theta_1'(0)|_{\beta=0}}$ called the coefficient of the heat transfer rate at the sheet.

3. Numerical solution

Transformed differential Eqs. (17), (22) and (23) with relevant boundary conditions (18) and (24) are highly nonlinear and possess no analytically solution and must be solved numerically by efficient Runge-Kutta method based on shooting technique with the help of software package Matlab. The higher order differential equations are converted into the set of eight first-order simultaneous equations and they require eight initial conditions to solve. Four initial conditions are known and remaining four missed initial conditions are obtained with the help of $f'(\infty)$, $f''(\infty)$, $\theta_1(\infty)$ and $\theta_2(\infty)$ by employing shooting technique. In shooting method, the boundary value problem is reduced to an initial value problem by assuming initial values. This method works by considering the boundary conditions as a function of multivariate of initial condition at some points, converting the boundary value problem to get the initial conditions. The boundary values calculated have to be matched with the real boundary values. An essential part of this method is to select the suitable finite value for η_∞. The maximum value of η_∞ is taken equal to 15 in order to achieve the far field boundary condition asymptotically.

4. Series solution based on genetic algorithm and Nelder-Mead method

4.1. Series solution

Our interest now is to find the series solutions of velocity $f(\eta)$ and temperature $\theta_1(\eta)$. For these solutions we write

$$f(\eta) = f_0(\eta) + \sum_{m=1}^{\infty} \frac{1}{m!} \left. \frac{\partial^m f(\eta, p)}{\partial p^m} \right|_{p=0} p^m \tag{28}$$

$$\theta_1(\eta) = \theta_{10}(\eta) + \sum_{m=1}^{\infty} \frac{1}{m!} \left. \frac{\partial^m \theta_1(\eta, p)}{\partial p^m} \right|_{p=0} p^m \tag{29}$$

Initial guesses f_0 and θ_{10} of $f(\eta)$ and $\theta_1(\eta)$ are chosen as

$$f_0(\eta) = S + 1 - \exp(-\eta), \theta_{10}(\eta) = \exp(-\eta) \tag{30}$$

The auxiliary linear operators are selected in the following forms:

$$L_f = \frac{d^3 f}{d\eta^3} - \frac{df}{d\eta} \tag{31}$$

$$L_{\theta 1} = \frac{d^3 \theta_1}{d\eta^3} - \theta_1 \tag{32}$$

The zeroth order deformation problems are constructed as

$$(1-q) L_f[\hat{f}(\eta, p) - f_0(\eta)] = q\hbar_f N_f[\hat{f}(\eta, p) - \hat{\theta}_1(\eta,\ \mathrm{p})] \tag{33}$$

$$(1-q) L_{\theta 1}[\hat{\theta}_1(\eta, p) - \theta_{10}(\eta)] = q\hbar_{\theta 1} N_{\theta 1}[\hat{f}(\eta, p) - \hat{\theta}_1(\eta,\ \mathrm{p})] \tag{34}$$

$$\hat{f}(\eta, p) = S|_{\eta=0}, \quad \left. \frac{\partial \hat{f}(\eta, p)}{\partial \eta} \right|_{\eta=0} = 1,$$
$$\left. \frac{\partial \hat{f}(\eta, p)}{\partial \eta} \right|_{\eta=\infty} = 0 \quad \frac{\partial \hat{\theta}_1(\eta, p)}{\partial \eta}|_{\eta=0} = 1, \quad \left. \frac{\partial \hat{\theta}_1(\eta, p)}{\partial \eta} \right|_{\eta=\infty} = 0 \tag{35}$$

in which the nonlinear operators N_f and $N_{\theta 1}$ are

$$\begin{aligned} &N_f[\hat{f}(\eta, p) - \hat{\theta}_1(\eta, q)] \\ &= \frac{\partial^3 \hat{f}(\eta, p)}{\partial \eta^3} - (1-\lambda_2)\left(\left(\frac{\partial \hat{f}(\eta, p)}{\partial \eta} \right)^2 - \hat{f}(\eta, p) \frac{\partial^2 \hat{f}(\eta, p)}{\partial \eta^2} \right) \\ &\quad + \gamma_1 \left(\left(\frac{\partial^2 \hat{f}(\eta, p)}{\partial \eta^2} \right)^2 - \hat{f}(\eta, p) \frac{\partial^4 \hat{f}(\eta, p)}{\partial \eta^4} \right) - (1+\lambda_2) \frac{2\beta \hat{\theta}_1(\eta, q)}{(\eta + \alpha_1)^4}, \end{aligned} \tag{36}$$

$$\begin{aligned} &N_{\theta 1}[\hat{f}(\eta, p) - \hat{\theta}_1(\eta, p)] \\ &= \frac{\partial^2 \hat{\theta}_1(\eta, p)}{\partial \eta^2} + Pr\left(\hat{f}(\eta, p) \frac{\partial \hat{\theta}_1(\eta, p)}{\partial \eta} - 2 \frac{\partial \hat{f}(\eta, p)}{\partial \eta} \hat{\theta}_1(\eta, p) \right) \\ &\quad + \frac{2\lambda\beta(\hat{\theta}_1(\eta, p) - \varepsilon)\hat{f}(\eta, p)}{(\eta + \alpha_1)^3} - 2\lambda \left(\frac{\partial \hat{f}(\eta, p)}{\partial \eta} \right)^2, \end{aligned} \tag{37}$$

when $p = 0$ and $p = 1$, we have

$$\hat{f}(\eta; 0) = f_0(\eta), \quad \hat{f}(\eta; 1) = f(\eta), \tag{38}$$

$$\hat{\theta}_1(\eta; 0) = \theta_{10}(\eta), \quad \hat{\theta}_1(\eta; 1) = \theta(\eta), \tag{39}$$

By Taylor theorem, we obtain

$$\hat{f}(\eta; p) = f_0(\eta) + \sum_{m=1}^{\infty} f_m(\eta) p^m, \tag{40}$$

$$\hat{\theta}_1(\eta; p) = \theta_{10}(\eta) + \sum_{m=1}^{\infty} \theta_{1m}(\eta) p^m, \tag{41}$$

$$f_m(\eta) = \frac{1}{m!} \left. \frac{\partial^m f(\eta, p)}{\partial \eta^m} \right|_{p=0} \tag{42}$$

$$\theta_{1m}(\eta) = \frac{1}{m!} \left. \frac{\partial^m \theta_1(\eta, p)}{\partial \eta^m} \right|_{p=0} \tag{43}$$

The auxiliary parameters are so properly chosen that the series (40) and (41) converge at $p = 1$, so we have

$$\hat{f}(\eta; p) = f_0(\eta) + \sum_{m=1}^{\infty} f_m(\eta), \tag{44}$$

$$\hat{\theta}_1(\eta; p) = \theta_{10}(\eta) + \sum_{m=1}^{\infty} \theta_{1m}(\eta), \tag{45}$$

The mth-order deformation problems are

$$N_f[f_m(\eta) - \chi_m f_{m-1}(\eta)] = \hbar_f \Re_m^f(\eta), \tag{46}$$

$$N_{\theta 1}[\theta_{1m}(\eta) - \chi_m \theta_{1m-1}(\eta)] = \hbar_{\theta 1} \Re_m^{\theta}(\eta), \tag{47}$$

$$\begin{aligned} &f_m(0) = 0, \quad f_m'(0) = 0, \quad f_m'(\infty) = 0 \\ &\theta_{1m}(0) = 0, \quad \theta_{1m}(\infty) = 0 \end{aligned} \tag{48}$$

$$\begin{aligned} \Re_m^f(\eta) = &f_{m-1}''' - (1+\lambda_2)\left[\sum_{k=0}^{m-1} (f_{m-1-k}' f_k' - f_{m-1-k} f_k'') \right] \\ &+ \gamma_1 \sum_{k=0}^{m-1} (f_{m-1-k}'' f_k'' - f_{m-1-k} f_k^{iv}) - (1+\lambda_2) \sum_{k=0}^{m-1} \left(\frac{2\beta\theta_{1m-1}}{(\eta + \alpha_1)^4} \right), \end{aligned} \tag{49}$$

$$\begin{aligned} \Re_m^{\theta 1}(\eta) = &Pr \sum_{k=0}^{m-1} (f_{m-1-k}\theta_{1k}' - 2f_{m-1-k}'\theta_{1k}) \\ &+ \frac{2\lambda\beta \sum_{k=0}^{m-1} (f_{m-1-k}\theta_{1k} - \varepsilon f_{m-1-k})}{(\eta + \alpha_1)^3} - 2\lambda \sum_{k=0}^{m-1} (f_{m-1-k}'' f_k''), \end{aligned} \tag{50}$$

$$\chi_m = \begin{cases} 0, & m \leqslant 1, \\ 1, & m > 1, \end{cases} \tag{51}$$

The general solution of (44) and (45) is

$$f_m(\eta) = f_m^*(\eta) + C_1 + C_2 \exp(\eta) + C_3 \exp(-\eta),$$

$$\theta_{1m}(\eta) = \theta_{1m}^*(\eta) + C_4 \exp(\eta) + C_5 \exp(-\eta),$$

where $f_m^*(\eta)$ and $\theta_{1m}^*(\eta)$ represent the special solution

4.2. Genetic algorithm and Nelder Mead method

Genetic algorithm (GA) is an optimization tool based on Darwinian evolution which has been developed in 1976, but its utilization in heat transfer problems has not been tested. In fact GA plays an important role when multiple parameters are involved. The main procedure is inspired by the Darwinian theory of evolution "The survival of the fittest." The genetic algorithm is a random search technique. Major advantage of GA is that the demand about computer memory for nonlinear problems is minimum. Genetic algorithm will be helpful for future even to get minimum and maximum solutions to satisfy

inequality relationships as well [30,31]. There are five main decision points in the procedure given below:

	Decision Points	(a)	(b)
1	Encoding technique ("chromosome structure")	Mechanism to encode solution	
2	Evaluation function ("environment")	Fitness function	
3	Selection procedure ("creation")		
4	Generating chromosome diversity ("evolution")	Crossover, mutation	
5	Parameter settings (practice and art)	Termination condition	(Random) initialization of population

There are several techniques for optimization such as analytical approach, downhill simplex method, gradient descent, and Newton's method. Moreover, the Nelder-Mead method is direct search simplex algorithm published in 1965 and is one of the most widely used methods for nonlinear unconstrained optimization. The Nelder-Mead method minimizes a nonlinear function of n real variables without taking any derivative. The function is evaluated at each point of the simplex structure formed by $(n + 1)$ points and the vertex with the highest value is replaced by a new point with a lower value. It continues until the minimum value of the function is achieved [32].

Table 1 Comparison of Nusselt number $-\theta_1'(0)$ for the case $\beta = \lambda = \lambda_2 = \gamma_1 = S = 0$.

Pr	Chen [7]	Abel et al. [29]	Numerical results	OHAM results
0.72	1.0885	1.0885	1.088527	1.088534
1	1.3333	1.3333	1.333333	1.333347
3	2.5097	–	2.509725	2.509729
10	4.7968	4.7968	4.796873	4.796874

5. Result and discussion

The purpose of the present article was to investigate the boundary layer flow and heat transfer of Jeffery fluid flow over a stretching surface with the effect of the magnetic dipole and suction/injection. Influence of various pertinent parameters is discussed with the help of figures and tables. The default values of the parameters for current work are considered as $Pr = 0.72$, $\beta = 0.2$, $\lambda_2 = 0.1$, $\gamma_1 = 0.2$ $\lambda = 0.01$, $S = 0.1$, $\varepsilon = 2.0$, $\alpha_1 = 1.0$. To check the efficiency of the numerical procedure, the present computational results for $-\theta_1'(0)$ are carried out for different values of *Pr* and compared with those reported by Chen [7] and Abel et al. [29] in Table 1 and found an excellent agreement. The numerical values of skin friction coefficient $-f''(0)$, Nusselt number $-\theta_1'(0)$ in PST and surface temperature $1/\theta_1(0)$ in PHF case are given for numerical solution and series solution based on GA and NM case for various values of the physical parameter presented in Table 2. This table is evident that Nusselt number for PST is directly proportional to Prandtl number, Deborah number, and suction/injection parameter, and inversely proportional to ferromagnetic interaction parameter, the ratio of relaxation and retardation times. Similarly, surface temperature for PHF case and skin friction coefficient is directly proportional to ferromagnetic interaction parameter, the ratio of relaxation and retardation times, and inversely proportional to Prandtl number, Deborah number. Table 3 identifies the fast convergence of optimal series solution. It has been observed that good convergence is obtained at even third iteration and excellent solution can be taken in only 5.463 sec.

Table 2 Skin friction coefficient $-f''(0)$, Nusselt number $-\theta_1'(0)$ and temperature function $\theta_1(0)$ for different values of *Pr*, β, λ_2, γ_1m *S* and λ.

Pr	β	λ_2	γ_1	*S*	λ	Numerical solution			Series solution based on GA and NM		
						$-f''(0)$	*PST* $-\theta_1'(0)$	PHF $1/\theta_1(0)$	$-f''(0)$	*PST* $-\theta_1'(0)$	PHF $1/\theta_1(0)$
1.0	0.2	0.1	0.2	0.1	0.01	1.0471	1.3959	0.7140	1.0470	1.3958	0.7138
2.0						1.0400	2.1185	0.4698	1.0399	2.1184	0.4697
3.0						1.0356	2.6850	0.3706	1.0357	2.6848	0.3705
3.0	2.0	0.1	0.2	0.1	0.01	1.3987	2.6459	0.3708	1.3986	2.6458	0.3706
	3.0					1.6043	2.6225	0.3708	1.6042	2.6223	0.3705
	4.0					1.8132	2.5975	0.3709	1.8131	2.5973	0.3708
3.0	0.2	0.1	0.2	0.1	0.01	1.0356	2.6850	0.3706	1.0355	2.6848	0.3704
		0.2				1.0815	2.6730	0.3723	1.0814	2.6728	0.3722
		0.3				1.1257	2.6614	0.3740	1.1255	2.6613	0.3739
3.0	0.2	0.1	0.1	0.1	0.01	1.0916	2.6711	0.3725	1.0914	2.6710	0.3724
			0.2			1.0356	2.6850	0.3706	1.0354	2.6849	0.3705
			0.3			0.9876	2.6969	0.3690	0.9875	2.6967	0.3689
3.0	0.2	0.1	0.2	0.1	0.01	1.0356	2.6850	0.3706	1.0352	2.6848	0.3705
				0.4		1.1379	3.2295	0.3080	1.1377	3.2293	0.3079
				0.6		1.2061	3.6327	0.2737	1.2060	3.6325	0.2736
3.0	0.2	0.1	0.2	0.1	0.4	1.0337	2.9108	0.2849	1.0335	2.9106	0.2848
					0.6	1.0327	3.0270	0.2407	1.0325	3.0269	0.2405
					0.8	1.0317	3.1434	0.1963	1.0316	3.1432	0.1961

Table 3 Series solution of velocity and temperature profile based on GA and NM.

Pr	β	λ_2	γ_1	*S*	λ	After 3rd Iteration				After 7th Iteration		
						η	Time	f'	θ_1	Time	f'	θ_1
0.72	0.2	0.1	0.2	0.1	0.01	0.0	3.689 s	1.0000	1.0000	5.463 s	1.0000	1.0000
						0.2		0.7951	0.7816		0.7950	0.7814
						0.4		0.6350	0.6176		0.6348	0.6175
						2.4		0.0869	0.1003		0.0868	0.1001
						5.0		0.0069	0.0127		0.0068	0.0125

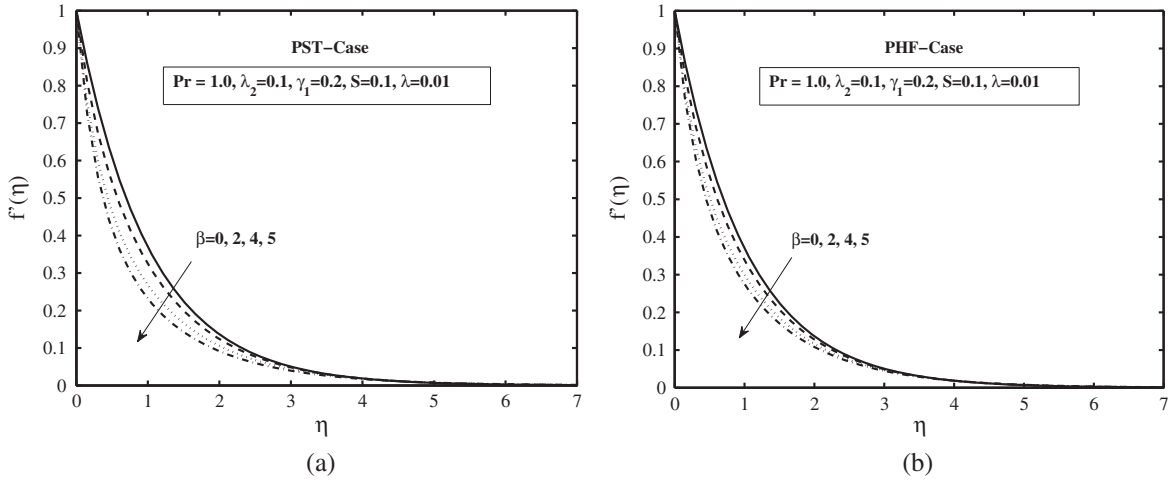

Figure 2 Effect of ferromagnetic interaction parameter β on velocity: (a) for PST and (b) for PHF.

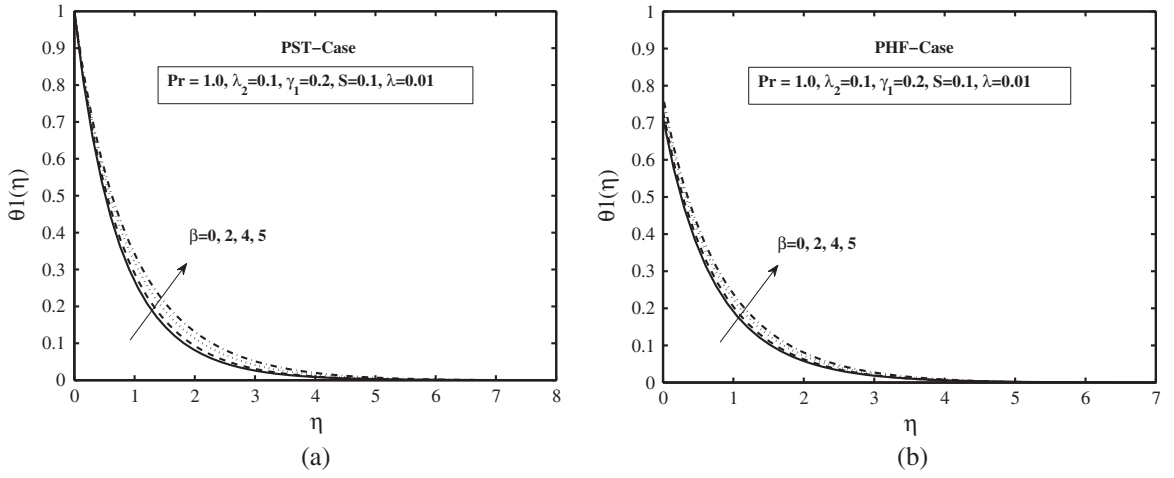

Figure 3 Effect of ferromagnetic interaction parameter β on temperature: (a) for PST and (b) for PHF.

The influence of applied external magnetic field due to magnetic dipole is demonstrated through ferromagnetic interaction parameter β. The existence of magnetic field acts as the delaying force on the velocity profile and then as β increases so does the delaying force and hence results in flattening the axial velocity $f'(\eta)$. This is because of the fact that variation of magnetic parameter leads to deviation of Lorentz force and this force produces a more resistance to the transport phenomena. Also noticed that in the presence of magnetic field, the velocity profile is less as compared with the hydrodynamic case ($\beta = 0$) for both PST and PHF cases as seen in Fig. 2(a) and (b). Because there is an intervention between the fluid motion and the action of the applied magnetic field, this kind of intervention reduces the velocity and increasing frictional heating involving within the fluid layers which are answerable for the enhancement in the thermal transport as cleared in Fig. 3 (a) and (b) for case PST and PHF.

Fig. 4(a) and (b) displays the influence of Deborah number (γ_1) on temperature profile for two types PST and PHF respectively. Increasing the values of Deborah number, there is a

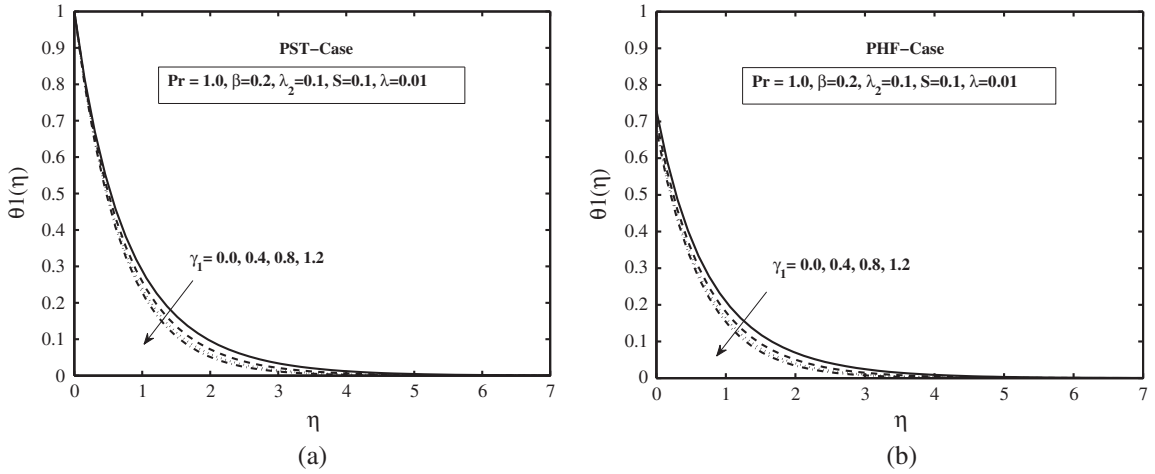

Figure 4 Effect of Deborah parameter γ_1 on velocity: (a) for PST and (b) for PHF.

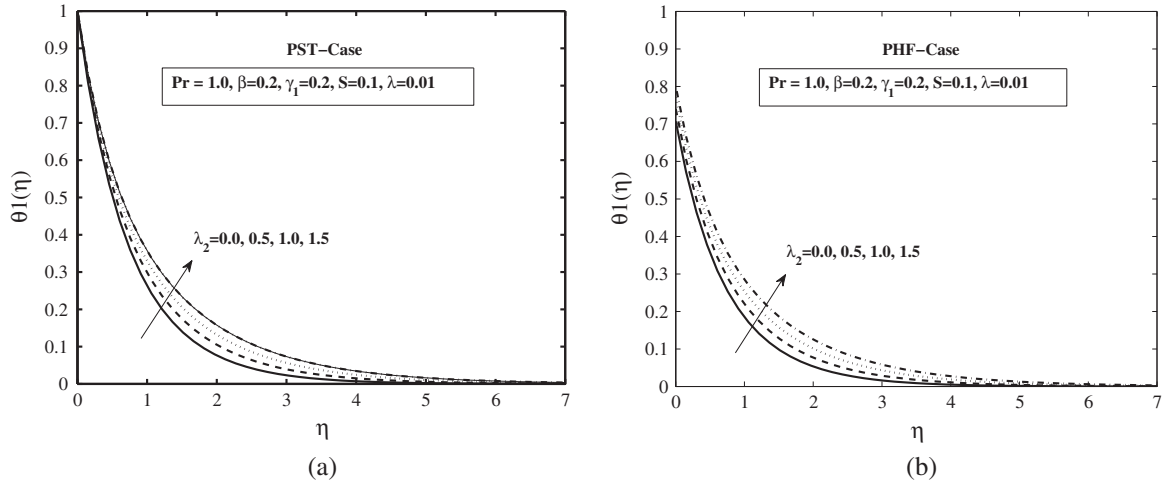

Figure 5 Effect of ratio of relaxation and retardation time λ_2 on temperature: (a) for PST and (b) for PHF.

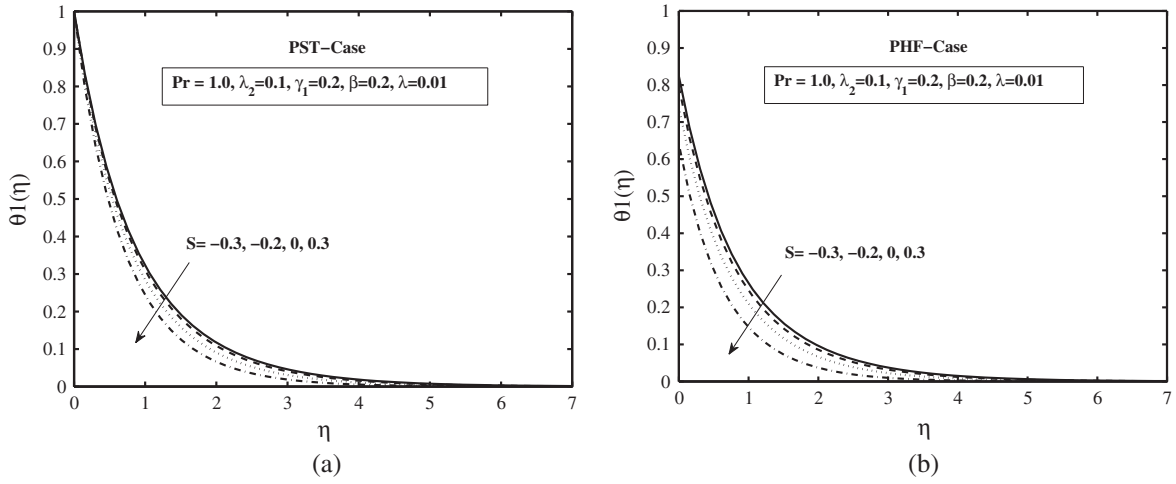

Figure 6 Effect of suction/injection S on temperature: (a) for PST and (b) for PHF.

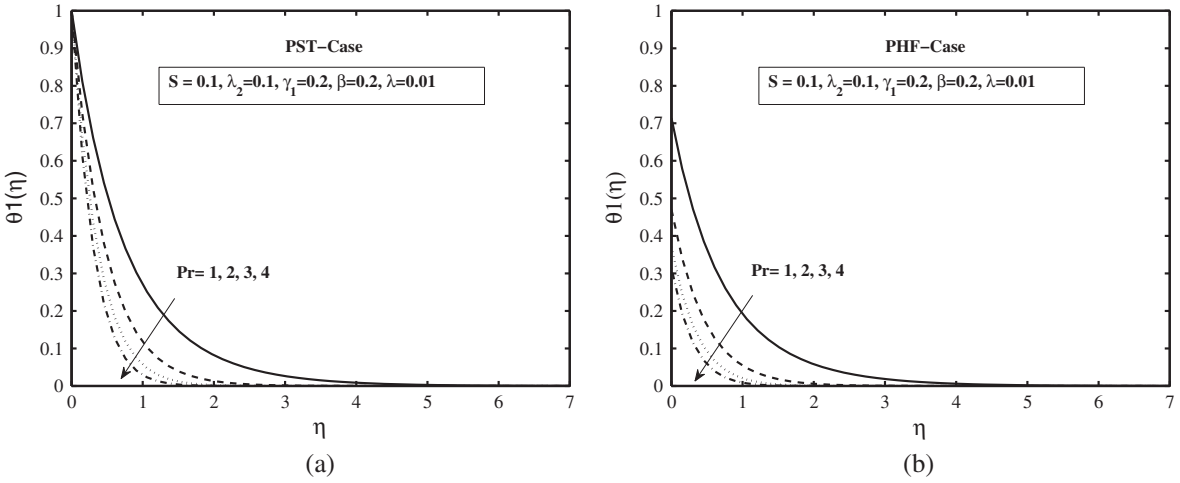

Figure 7 Effect of *Pr* on temperature: (a) for PST and (b) for PHF.

decrease in temperature profile θ_1 for both types PST and PHF. Physically γ_1 is proportional to retardation time λ_1; hence, a large retardation time of any material makes it less viscous, which may result in an increase in its motion, which consequently weakens the thermal boundary layer thickness and lower temperature profile.

Fig. 5(a) and (b) portrays the effect of the ratio of relaxation to retardation time parameter λ_2 on temperature profile θ_1. From figures, it observed that temperature profile is gradually increasing with an increase in the value of λ_2 for both cases PST and PHF. An increase in λ_2 implies to an increase in relaxation time and decrease in retardation time. This change in relaxation and retardation times elucidates the rise in temperature and thicker thermal boundary layer thickness.

Fig. 6(a) and (b) represents the influence of suction/injection parameter (S) on temperature profile for both cases PST and PHF. It is evident temperature profile depreciates with increasing suction parameter ($S > 0$) whereas for injection ($S < 0$) opposite behavior is noted. Here negative values signify the injection and positive values signify the suction. Moreover, the thermal boundary layer thickness reduces with the increase in S for both PST and PHF cases.

Fig. 7(a) and (b) draws to analyze the effect of Prandtl number on temperature profile θ_1. It is seen that temperature decreases with respect to *Pr* for both PST and PHF cases. This is due to the fact that fluid has relatively lower thermal conductivity for a large value of Prandtl number, which reduces the conduction and thermal boundary layer thickness, as a result temperature decreases.

Fig. 8(a) and (b) highlights the skin friction coefficient and Nusselt number with the variation of ferromagnetic interaction parameter β for different values of Prandtl number *Pr*. It is evident that skin friction coefficient increases by an increase in β whereas depreciates for *Pr*. Also by increasing the value of Prandtl number *Pr* there is an increase in Nusselt number, as the fluid with large Prandtl number *Pr* has higher heat capacity and hence increases the heat transfer rate seen in Fig. 8(b).

Fig. 9(a) and (b) illustrates the effect of suction parameter S on skin friction coefficient and Nusselt number with the variation of β. From Fig. 9(a) it can be observed that the graph

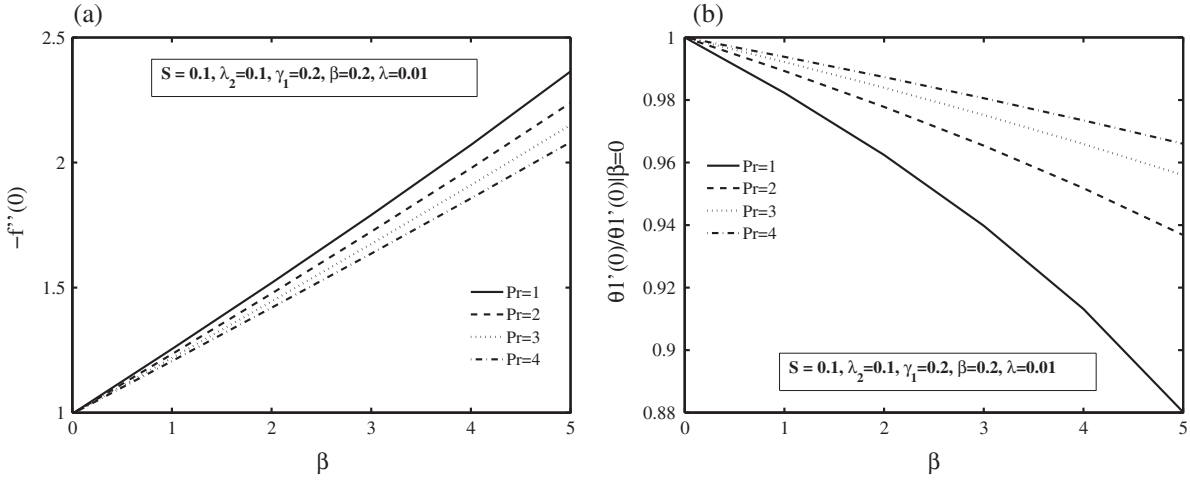

Figure 8 (a) Skin friction coefficient and (b) Nusselt number with the variation of ferromagnetic interaction parameter β for different values of Prandtl number *Pr*.

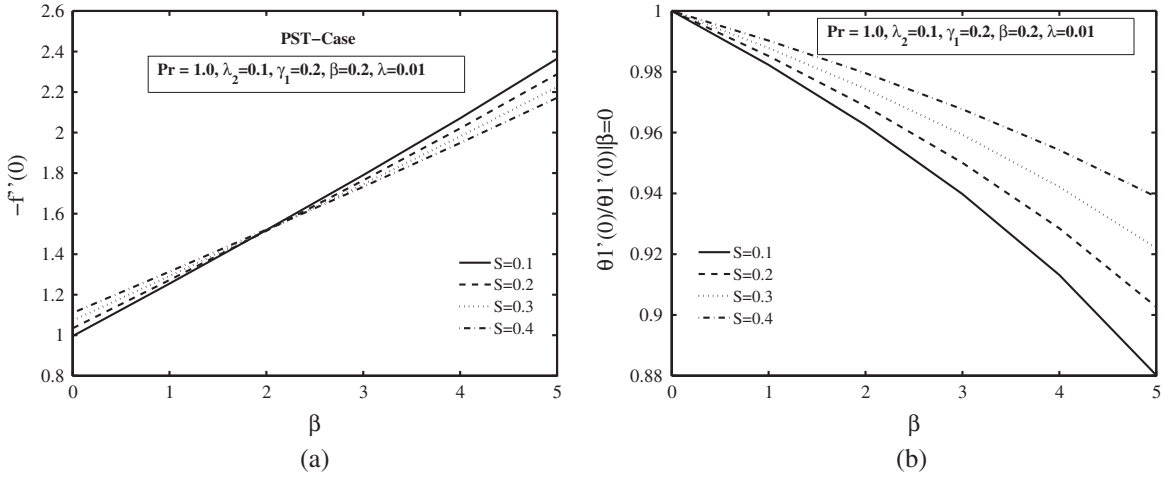

Figure 9 (a) Skin friction coefficient and (b) Nusselt number with the variation of ferromagnetic interaction parameter β for different values of $S > 0$.

of skin friction coefficient increases for $\beta > 2$ and decreases for $\beta < 2$. Also for $S > 0$ the rate of heat transfer is enhanced, whereas the reverse trend is occurred for β as shown in Fig. 9(b).

6. Concluding remarks

Fourth-fifth order Runge-Kutta numerical method with shooting technique and series solution based on GA and NM is employed on incompressible boundary layer flow and heat transfer of a Jeffrey fluid past a linearly stretching sheet with the effect of magnetic dipole for two types of heating process, namely prescribed surface temperature (PST) and prescribed heat flux (PHF). The results of several physical parameters such as ferromagnetic interaction parameter (β), Deborah number (γ_1), ratio of relaxation to retardation times (λ_2), suction/injection parameter (S), Prandtl number (Pr) on velocity and temperature profiles are examined and discussed graphically in details. Finally, some important observations based on the present study are as follows:

- Ferromagnetic interaction parameter β decreases velocity and increases temperature.
- The effect of Prandtl number Pr is to decrease the temperature for both PST and PHF cases.
- The influence of suction/injection parameter is to decrease the thermal boundary layer thickness.
- Skin friction coefficient is an increasing function of β, λ_2, S and decreasing function of γ_1, Pr.
- Local Nusselt number has increasing effect with increase in Deborah number, suction/injection parameter and Prandtl number, while opposite nature is seen for surface temperature.

References

[1] H. Blasius, Grenzschichten in Flussigkeiten mit kleiner Reibung, Z. Angew. Math. Phys. 56 (1908) 1–37.
[2] B.C. Sakiadis, Boundary-layer behaviour on continuous solid surfaces. I. Boundary-layer equations for two-dimensional and axisymmetric flow, AIChE J. 7 (1961) 26–28.
[3] L.J. Crane, Flow past a stretching plate, Z. Angew. Math. Phys. 21 (1970) 645–647.
[4] P.S. Gupta, A.S. Gupta, Heat and mass transfer on a stretching sheet with suction or blowing, Can. J. Chem. Eng. 55 (1977) 744–746.
[5] P.D. Ariel, Extended homotopy perturbation method and computation of flow past a stretching sheet, Comput. Math. Appl. 58 (2009) 2402–2409.
[6] A. Chakrabarti, A.S. Gupta, Hydromagnetic flow and heat transfer over a stretching sheet, Quart. J. Appl. Math. 37 (1979) 73–78.
[7] C.H. Chen, Laminar mixed convection adjacent to vertical, continuously stretching sheets, Heat Mass Transf. 33 (1998) 471–476.
[8] A. Zeeshan, A. Majeed, Non Darcy mixed convection flow of magnetic fluid over a permeable stretching sheet with ohmic dissipation, J. Magn. 21 (2016) 153–158.
[9] P.V.S. Narayana, D.H. Babu, Numerical study of MHD heat and mass transfer of a Jeffrey fluid over a stretching sheet with chemical reaction and thermal radiation, J. Taiwan Inst. Chem. Eng. 59 (2016) 18–25.
[10] H. Xu, S.J. Liao, Laminar flow and heat transfer in the boundary layer of non-Newtonian fluids over a stretching flat sheet, Comput. Math. Appl. 57 (2009) 1425–1431.
[11] A. Ishak, K. Jafar, R. Nazar, I. Pop, MHD stagnation point flow towards a stretching sheet, Physica A 388 (2009) 3377–3383.
[12] B. Sahoo, Flow and heat transfer of a non-Newtonian fluid past a stretching sheet with partial slip, Commun. Nonlinear Sci. Numer. Simul. 15 (2010) 602–615.
[13] N. Sandeep, C. Sulochana, A. Isaac Lare, Stagnation-point flow of a Jeffrey nanofluid over a stretching surface with induced magnetic field and chemical reaction, Int. J. Eng. Res. Africa 20 (2016) 93–111.
[14] C.S.K. Raju, N. Sandeep, M. Gnaneswara Reddy, Effect of nonlinear thermal radiation on 3D Jeffrey fluid flow in the presence of homogeneous-heterogeneous reactions, Int. J. Eng. Res. Africa 21 (2016) 52–68.
[15] M.M. Rashidi, M. Ali, N. Freidoonimehr, B. Rostami, M.A. Hossain, Mixed convective heat transfer for MHD viscoelastic fluid flow over a porous wedge with thermal radiation, Adv. Mech. Eng. 6 (2014) 735939.
[16] T. Hayat, R. Sajjad, S. Asghar, Series solution for MHD channel flow of a Jeffery fluid, Commun. Nonlinear Sci. Numer. Simul. 15 (2010) 2400–2406.

[17] T. Hayat, M. Awais, S. Obaidat, Three-dimensional flow of a Jeffery fluid over a linearly stretching sheet, Commun. Nonlinear Sci. Numer. Simul. 17 (2012) 699–707.
[18] I.L. Animasaun, C.S.K. Raju, N. Sandeep, Unequal diffusivities case of homogeneous–heterogeneous reactions within viscoelastic fluid flow in the presence of induced magnetic-field and nonlinear thermal radiation, Alexandria Eng. J. 52 (2) (2016) 1595–1606.
[19] S. Nadeem, R.U. Haq, Z.H. Khan, Numerical solution of non-Newtonian nanofluid flow over a stretching sheet, Appl. Nanosci. 4 (2014) 625–631.
[20] M.M. Rashidi, E. Erfani, Analytical method for solving steady MHD convective and slip flow due to a rotating disk with viscous dissipation and Ohmic heating, Eng. Comput. 29 (2012) 562–579.
[21] M.Y. Malik, I. Zehra, S. Nadeem, Numerical treatment of Jeffrey fluid with pressure-dependent viscosity, Int. J. Numer. Meth. Fluids 68 (2012) 196–209.
[22] C.S.K. Raju, M.J. Babu, N. Sandeep, Chemically reacting radiative MHD Jeffrey nanofluid flow over a cone in porous medium, Int. J. Eng. Res. Africa 19 (2016) 75–90.
[23] N. Sandeep, B. Rushi Kumar, M.S. Jagadeesh Kumar, A comparative study of convective heat and mass transfer in non-Newtonian nanofluid flow past a permeable stretching sheet, J. Mol. Liq. 212 (2015) 585–591.
[24] M.H. Abolbashari, N. Freidoonimehr, F. Nazari, M.M. Rashidi, Entropy analysis for an unsteady MHD flow past a stretching permeable surface in nano-fluid, Powder Technol. 267 (2014) 256–267.
[25] M. Narayana, L.R. Titus, A. Abraham, P. Sibanda, Modelling micropolar ferromagnetic fluid flow due to stretching of an elastic sheet, Afrika Matematika 25 (2014) 667–679.
[26] H.I. Andersson, O.A. Valnes, Flow of a heated Ferrofluid over a stretching sheet in the presence of a magnetic dipole, Acta Mech. 128 (1998) 39–47.
[27] S. Nadeem, N.S. Akbar, Peristaltic flow of a Jeffrey fluid with variable viscosity in an asymmetric channel, Zeitschrift für Naturforschung A 64 (2009) 713–722.
[28] L.S. Titus, A. Abraham, Ferromagnetic liquid flow due to gravity-aligned stretching of an elastic sheet, J. Appl. Fluid Mech. 8 (2015) 591–600.
[29] M.S. Abel, E. Sanjayanand, M.M. Nandeppanavar, Viscoelastic MHD flow and heat transfer over a stretching sheet with viscous and ohmic dissipations, Commun. Nonlinear Sci. Numer. Simul. 13 (2008) 1808–1821.
[30] N.E. Mastorakis, Numerical solution of non-linear ordinary differential equations via collocation method (finite elements) and genetic algorithms, in: Proceedings of the 6th WSEAS Int. Confer. on Evolu. Comput. Lisbon, Portugal, 2005.
[31] C.I. Hung, Y.L. Zong, Double side approach method to obtain solutions for transient nonlinear heat conduction using genetic algorithms, Appl. Math. Comput. 133 (2002) 431–444.
[32] N.E. Mastorakis, Unstable ordinary differential equations: solution via genetic algorithms and the method of Nelder-Mead, Proceedings of the 6th WSEAS Int. Conf. on Systems Theory and Scientific Computation, Elounda, Greece, August, vol. 5, 2006, p. 1276.